

Accepted Manuscript

The influence of structure and surface chemistry of carbon materials on the decomposition of hydrogen peroxide

Rui S. Ribeiro, Adrián M.T. Silva, José L. Figueiredo, Joaquim L. Faria, Helder T. Gomes

PII: S0008-6223(13)00494-6

DOI: <http://dx.doi.org/10.1016/j.carbon.2013.06.001>

Reference: CARBON 8088

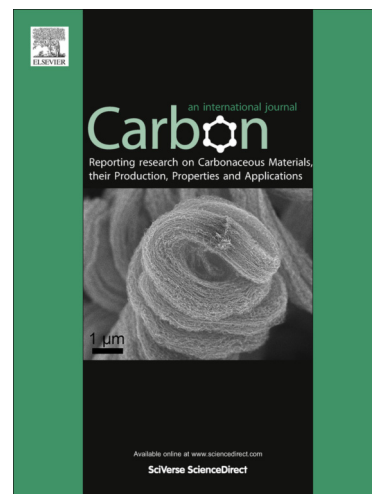
To appear in: *Carbon*

Received Date: 4 February 2013

Accepted Date: 1 June 2013

Please cite this article as: Ribeiro, R.S., Silva, A.M.T., Figueiredo, J.L., Faria, J.L., Gomes, H.T., The influence of structure and surface chemistry of carbon materials on the decomposition of hydrogen peroxide, *Carbon* (2013), doi: <http://dx.doi.org/10.1016/j.carbon.2013.06.001>

This is a PDF file of an unedited manuscript that has been accepted for publication. As a service to our customers we are providing this early version of the manuscript. The manuscript will undergo copyediting, typesetting, and review of the resulting proof before it is published in its final form. Please note that during the production process errors may be discovered which could affect the content, and all legal disclaimers that apply to the journal pertain.



The influence of structure and surface chemistry of carbon materials on the decomposition of hydrogen peroxide

Rui S. Ribeiro^a, Adrián M.T. Silva^b, José L. Figueiredo^b, Joaquim L. Faria^b, Helder T. Gomes^{a,b,*}

^a *Department of Chemical and Biological Technology, School of Technology and Management, Polytechnic Institute of Bragança, Campus de Santa Apolónia, 5300-857 Bragança, Portugal.*

^b *LCM - Laboratory of Catalysis and Materials - Associate Laboratory LSRE/LCM, Faculdade de Engenharia, Universidade do Porto, Rua Dr. Roberto Frias, 4200-465 Porto, Portugal.*

*Corresponding author. Tel.: +351 273 303 110; Fax: +351 273 313 051.

E-mail address: htgomes@ipb.pt (H.T. Gomes)

Abstract

Carbon materials with different structural and chemical properties, namely activated carbons, carbon xerogels, carbon nanotubes, graphene oxide, graphite and glycerol-based carbon materials, were tested under different operating conditions for their ability to catalyse hydrogen peroxide (H_2O_2) decomposition in aqueous solutions. Activated carbons treated with concentrated sulphuric acid (ACS) are the most active catalytic materials for H_2O_2 decomposition in most of the conditions studied, due to the presence of sulphur containing functional groups at their surface. In addition, ACS proved to be a stable catalyst in reutilization tests for H_2O_2 decomposition. Methanol was used as selective scavenger of hydroxyl radicals (HO^\bullet), to show that activated carbons with a markedly basic character lead to the highest yield of HO^\bullet formed during the H_2O_2 decomposition process (14%, after 150 min of reaction). Overall, from the mechanistic interpretation of H_2O_2 decomposition, it is concluded that the presence of sulphur containing functional groups at the surface of the activated carbons improves the removal of H_2O_2 in aqueous solutions, but, on the other hand, the selective decomposition of H_2O_2 via HO^\bullet formation is enhanced by the presence of basic active sites on the carbon surface.

1. Introduction

Hydrogen peroxide (H_2O_2) – at room temperature, a colourless liquid with a bitter taste – is usually available in dilute form (3% to 10%) for household use, and in concentrated form (higher than 30%) for industrial applications [1]. Commercially, H_2O_2 is mostly used in disinfectants and deodorants, whereas in industry it is also considered as a bleaching agent for textiles and paper production, as a component of rocket fuels, as a reactant for producing foam rubber and as an oxidizing agent in wastewater treatments and in several other processes [1-3]. H_2O_2 is naturally unstable, since it decomposes readily to oxygen and water with release of heat, therefore a stabilizer (*e.g.* acetanilide) is usually added to the H_2O_2 formulation with the aim of slowing down the rate of its spontaneous decomposition [1]. Thus, some industrial wastewaters fed to biological processes contain significant amounts of H_2O_2 and, in some particular cases, traces of H_2O_2 can also be found in municipal wastewaters. Since H_2O_2 leads to the destruction of bacterial cells [4], the efficiency of the biological processes tends to decrease when H_2O_2 is in solution and, in such case, appropriate technologies for the removal of H_2O_2 from wastewaters should be applied.

On the other hand, selective decomposition of H_2O_2 through the formation of highly reactive hydroxyl radicals (HO^\bullet) is important in some advanced oxidation processes (AOP) used for wastewater treatment, such as in the case of the so-called catalytic wet peroxide oxidation (CWPO) process, which is a liquid phase remediation technology often applied before a biological treatment and involving the use of H_2O_2 and a suitable catalyst [2]. CWPO is particularly attractive due to the use of mild conditions in comparison to other AOP [5] and, recently, it has been shown that activated carbon materials can act as metal-free catalysts for the CWPO of organic pollutants in aqueous solution [6-9], thus avoiding the presence of metallic species at the end of treatment, a typical drawback related with the use of homogeneous or unstable heterogeneous metallic catalysts [10, 11]. Therefore, in this

particular case, the complete and selective decomposition of H_2O_2 into HO^\bullet by means of metal-free carbon materials is desired.

In the present work, (i) the decomposition of H_2O_2 using carbon materials as catalysts as well as (ii) the yield of HO^\bullet formed during the decomposition process were analysed. Carbon materials with different structural and chemical properties were tested: a commercial activated carbon (Norit ROX 0.8, used as received and chemically modified by liquid phase and thermal treatments), a carbon xerogel prepared by polycondensation of resorcinol with formaldehyde, a commercial multi-walled carbon nanotube (Sigma-Aldrich), graphene oxide, natural graphite and a glycerol-based carbon material prepared by partial carbonization of glycerol in concentrated sulphuric acid.

This study will be important when using carbon materials for the removal of H_2O_2 from industrial (or even municipal) wastewaters fed to biological processes and, for this reason, a wide range of operating conditions was considered, with subsequent assessment of the suitability of the best catalyst to be used at the industrial scale. In addition, the determination of HO^\bullet formed during the catalytic H_2O_2 decomposition process was assessed, and a mechanism was proposed for the decomposition of H_2O_2 via formation of HO^\bullet in parallel with the decomposition of H_2O_2 into other species, thus allowing for the correct interpretation of the experimental data, which is relevant when dealing with AOPs based on H_2O_2 .

2. Materials and methods

2.1. Reactants

Resorcinol (99 wt.%), iron (III) nitrate nonahydrate (98 wt.%), formaldehyde solution (37 wt.% in water, stabilized with 15 wt.% methanol), methanol (99.8 wt.%), titanium (IV) oxysulphate (15 wt.% in dilute sulphuric acid, 99.99%) and hydrochloric acid (37%) were purchased from Sigma-Aldrich. H_2O_2 (30% w/v) and sodium hydroxide (98 wt.%) were

obtained from Panreac. Sulphuric acid (96–98 wt.%), nitric acid (65 wt.%) and urea (65 wt.%) were obtained from Riedel-de-Haën. Glycerol (99 wt.%) was obtained from Alfa Aesar. Potassium permanganate (99%) was supplied by Merck. All chemicals were used as received without further purification. Distilled water was used throughout the work.

2.2. Carbon materials

Six types of carbon materials, with different structural characteristics, were initially considered in this work: (i) the commercial activated carbon Norit ROX 0.8 (AC), (ii) a carbon xerogel (CX), (iii) a commercial sample of multi-wall carbon nanotubes (> 90% carbon basis, O.D. × I.D. × L: 10-15 nm × 2-6 nm × 0.1-10 μm) obtained from Sigma-Aldrich, ref. 677248 (CNT), (iv) graphene oxide (GO) obtained from (v) natural graphite (particle size ≤ 20 μm, 99.9995% purity, obtained from Sigma-Aldrich) and (vi) a glycerol-based carbon material (GBCM).

AC is a commercial acid washed extruded activated carbon produced by steam activation and, as specified by the supplier, characterized by a high purity and an ash content of only 3 wt.% (0.02 wt.% Fe).

CX was prepared by polycondensation of resorcinol with formaldehyde (with a molar ratio of 1:2), following the procedure described elsewhere [12]. 9.91 g of resorcinol were added to 18.8 mL of deionised water in a glass flask. After complete dissolution, 13.5 mL of formaldehyde solution were also added. In order to achieve the desired initial pH of the precursor solution (6.1), sodium hydroxide solution was added dropwise under continuous stirring and pH monitoring. The gelation step was allowed to proceed at 358 K during 3 days. After this period the gel was dark red and the consistency of the material allowed the sample to be shaped as desired. The gel was further dried in oven from 333 K to 423 K during several

days, defining a heating ramp of 20 K day⁻¹. After drying, the gel was pyrolyzed at 1073 K under a nitrogen flow (100 cm³ min⁻¹) in a tubular vertical oven.

CNT are commercial carbon nanotubes (Arkema Inc., Graphistrength[®] C100) with contents of alumina and iron oxide under 7 wt.% and 5 wt.%, respectively, and without detectable free amorphous carbon [13-15].

GO was obtained from natural graphite by using the modified Hummers method [16, 17], as described elsewhere [18]. 50 mL of concentrated sulphuric acid was added gradually with stirring and cooling to a 500 mL flask containing 2 g of graphite. Then, 6 g of potassium permanganate were added slowly to the mixture. The suspension was continuously stirred for 2 h at 308 K. After that, it was cooled in an ice bath and subsequently diluted by 350 mL of distilled water. Afterwards, H₂O₂ (30% w/v) was added in order to reduce residual permanganate to soluble manganese ions, a bright yellow colour appearing in the suspension. The oxidized material was purified with an hydrochloric acid solution (10 wt.%) and the suspension was then filtered, washed several times with distilled water until the neutrality of the rinsing water was reached, and dried at 333 K for 24 h to obtain graphite oxide. The resulting material was dispersed in a given volume of water and sonicated in an ultrasound bath (ultrasonic processor UP400S, 24 kHz) for 1 h. The sonicated dispersion was centrifuged for 20 min at 3000 rpm to remove unexfoliated graphite oxide particles from the supernatant, GO being obtained by this way.

GBCM was prepared by partial carbonization of glycerol adapting the procedure described elsewhere [19]. A mixture of glycerol (10 g) and concentrated sulphuric acid (40 g) was gently heated to 453 K and left at that temperature for 20 min to allow in situ partial carbonization and sulfonation. During heating, the liquid gradually got darker and, at 418 K, the mixture started to foam intensely, quickly thickened and gained density resulting in a

black solid, which was then cooled, washed and filtered in warm water until the neutrality of the rinsing waters was reached.

Except for CNT, GO and graphite, all other materials were ground to particle sizes in the range 0.106-0.250 mm.

2.2.1. Modified carbon materials

The original powdered AC was modified by liquid phase, thermal and hydrothermal treatments, resulting in the production of four additional activated carbon samples, following the procedures reported elsewhere [6, 20]: a 50 g L⁻¹ mixture containing AC in concentrated sulphuric acid solution (18 mol L⁻¹) was kept for 3 h at 423 K in a 500 mL round-bottom flask heated by an oil bath; the recovered solids were thoroughly washed with distilled water until the neutrality of the rinsing waters was reached, and further dried in an oven for 18 h at 383 K, resulting in ACS materials. A 50 g L⁻¹ mixture containing AC in nitric acid (5 mol L⁻¹) was kept for 3 h at boiling temperature, the recovered solids washed and further dried in oven for 18 h at 383 K, resulting in ACN materials; a 40 g L⁻¹ mixture containing ACN in urea solution (1 mol L⁻¹) was kept in a 125 mL stainless steel autoclave under autogenous pressure at 473 K for 2 h, the recovered samples being thoroughly washed with distilled water until the neutrality of the rinsing waters was reached, and further dried overnight in oven at 383 K, resulting in the ACNU materials; a gas phase thermal treatment was then applied, in which 1 g of ACNU was heated under a nitrogen flow (100 cm³ min⁻¹) at 393 K, 673 K and 873 K during 60 min at each temperature and then at 1073 K for 240 min, using a heating ramp of 2 K min⁻¹, resulting in the ACNUT materials.

2.3. Characterization techniques

The textural properties of all tested materials were determined from N₂ adsorption-desorption isotherms at 77 K, obtained in a Quantachrome NOVA 4200e

adsorption analyser. The specific surface area (S_{BET}) was calculated using the BET method, the non-microporous surface area ($S_{\text{Non-mic}}$) and the micropore volume (V_{Mic}) were obtained by the t-method. The single point adsorption total pore volume (V_{Total}) was calculated at $P/P_0 = 0.995$.

Temperature Programmed Desorption (TPD) analysis was performed in a fully automated AMI-300 Catalyst Characterization Instrument (Altamira Instruments), equipped with a quadrupole mass spectrometer (Dymaxion, Ametek). The carbon sample (0.10 g) was placed in a U-shaped quartz tube inside an electrical furnace and heated at 5 K min^{-1} up to 1073 K using a constant flow rate of helium ($25 \text{ cm}^3 \text{ min}^{-1}$). The mass signals $m/z = 28$ and 44 were monitored during the thermal analysis, the corresponding TPD spectra being obtained. CO and CO₂ were calibrated at the end of each analysis with the respective gases [21].

The point of zero charge (*PZC*) was determined by the pH drift method following the procedure described elsewhere [22]. Five solutions with varying initial pH were prepared using HCl and NaOH solutions (0.02 mol L^{-1} and 1.0 mol L^{-1}) and NaCl (0.01 mol L^{-1}) as electrolyte; 50 mL of each solution was contacted with 0.15 g of carbon sample and the suspension stirred for 24 h before the equilibrium pH was measured. The *PZC* value of each carbon sample was determined by intercepting the obtained final pH vs. initial pH curve with the straight line final pH = initial pH [23, 24].

The concentration of acidic active sites at the materials surface was determined as reported in recent works developed by our group [6, 25], by adding 0.2 g of each sample to 25 mL of a 0.02 mol L^{-1} NaOH solution. The resulting suspension was left under stirring for 48 h at room temperature. After filtration, to remove the solid material, the unreacted OH⁻ was titrated with a 0.02 mol L^{-1} HCl solution. The initial concentration of acidic functionalities was then calculated by the difference between the amount of NaOH initially present in the suspension and the amount of NaOH determined by titration, and finally dividing this value by the mass

of material. The concentration of basic active sites was determined in a similar way, this time by adding the carbon sample to a 0.02 mol L^{-1} HCl solution and titrating the solution obtained after stirring and filtration with a 0.02 mol L^{-1} NaOH solution. Phenolphthalein was used as indicator in both titrations.

2.4. H_2O_2 decomposition experimental procedures

Two distinct experimental procedures were considered during this work: experiments monitoring the concentration of H_2O_2 and experiments monitoring the amount of oxygen formed, either with or without the presence of methanol (20 g L^{-1}), which acts as a trap for HO^\bullet . These experimental procedures allow us to discriminate between alternative surface catalysed H_2O_2 decomposition pathways [26].

In both experimental procedures, the H_2O_2 decomposition reactions were performed in a 500 mL well-stirred (600 rpm) glass reactor, equipped with a condenser, a temperature measurement thermocouple, a pH measurement electrode and a sample collection port. The reactor was loaded with 250 mL of distilled water and heated by immersion in a water bath monitored by a temperature controller. Upon stabilization at the desired temperature, the solution pH was adjusted by means of H_2SO_4 and NaOH solutions. Following the conditions used in recent works developed by our group [6, 8, 25], a calculated volume of H_2O_2 (6 wt.%) was then injected into the system, in order to reach a H_2O_2 concentration ($[\text{H}_2\text{O}_2]$) of 34.6 mmol L^{-1} and, after its complete mixing, the catalyst was added to the solution, that moment being considered as $t_0 = 0 \text{ min}$. Typical experiments were performed during 150 min, at $T = 323 \text{ K}$, $\text{pH} = 3$ and catalyst load = 0.1 g L^{-1} . Iron nitrate nonahydrate was used as Fe^{3+} source in a homogeneous H_2O_2 decomposition run. In the H_2O_2 decomposition experiments monitoring the concentration of H_2O_2 , the samples for analysis were periodically withdrawn through the sample collection port. In the H_2O_2 decomposition experiments monitoring the

amount of oxygen formed, the sample collection port was kept closed and the gas was continuously collected through a flexible hose attached to the neck of the condenser.

2.5. Analytical methods

The concentration of H_2O_2 was followed by a colorimetric method [27], adapted from the literature [28]. 1 mL of filtered sample was added to 1 mL of sulphuric acid solution (0.5 mol L^{-1}) in a 20 mL volumetric flask, to which 0.1 mL of titanium oxysulfate was added. The resulting mixture was diluted with distilled water and further analysed by UV-vis spectrophotometry (T70 spectrometer, PG Instruments, Ltd.).

The formation of oxygen was volumetrically quantified. An inverted graduated cylinder immersed in a water bath at room temperature was connected to the reactor through a flexible hose. The amount of oxygen formed was initially quantified through the water displacement in the inverted graduated cylinder, being then corrected considering the pressure of the water column and the differences between room and reaction temperatures.

Selected experiments were performed in duplicate, in order to assess reproducibility and error of the experimental results obtained through the analytical methods used to quantify oxygen and H_2O_2 . The error was less than 3% for both methods.

2.6. H_2O_2 decomposition kinetics

In order to evaluate the global H_2O_2 decomposition rate, a first order kinetic law was used [26, 29, 30], Equation 1, where k_d represents the apparent H_2O_2 global decomposition rate constant (min^{-1}).

$$r_d = -\frac{d[\text{H}_2\text{O}_2]}{dt} = k_d[\text{H}_2\text{O}_2] \quad (1)$$

3. Results and discussion

3.1. Textural and surface chemistry characterization

The textural properties of the tested carbon materials, determined as described in Section 2.3, are summarized in Table 1. As observed, AC is essentially a microporous material ($V_{\text{Mic}}/V_{\text{Total}}$ higher than 0.5), characterized by a high surface area and possessing the highest value of S_{BET} amongst the six types of carbon materials initially considered in this work. In the opposite, GO, graphite and GBCM are non-porous materials, with V_{Total} ranging from $0.02 \text{ cm}^3 \text{ g}^{-1}$ to $0.04 \text{ cm}^3 \text{ g}^{-1}$. Furthermore, GBCM presents the lowest S_{BET} amongst the initial tested carbon materials. As expected, CNT are non-microporous materials, with $V_{\text{Mic}} = 0 \text{ cm}^3 \text{ g}^{-1}$. Nevertheless, CNT present a significant specific surface area and a V_{Total} above $1 \text{ cm}^3 \text{ g}^{-1}$, which is primarily due to adsorption on the external surface of the tubes [31] and to adsorption on the surface of the inner cavities of some open CNT (the measured specific surface area is slightly higher than the calculated geometric area, suggesting that a small fraction of CNT have some open ends). CX is a typical mesoporous material, with a ratio $V_{\text{Mic}}/V_{\text{Total}}$ of 0.17.

Regarding the activated carbon samples produced by modification of the original AC, it is concluded from Table 1 that the treatment with concentrated sulphuric acid (ACS) does not affect the textural properties of AC and that the successive chemical treatments with concentrated nitric acid (ACN) and urea (ACNU), as well as the thermal treatment (ACNUT), mainly lead to a slight development of mesopores, since the $S_{\text{Non-mic}}$ value successively increases as the materials are subjected to new treatments, without noteworthy modification of the microporosity.

Table 1. Specific surface area (S_{BET} , $\pm 10 \text{ m}^2 \text{ g}^{-1}$), non-microporous surface area ($S_{\text{Non-mic}}$, $\pm 10 \text{ m}^2 \text{ g}^{-1}$), total pore volume (V_{Total} , $\pm 0.01 \text{ cm}^3 \text{ g}^{-1}$) and micropore volume (V_{Mic} , $\pm 0.01 \text{ cm}^3 \text{ g}^{-1}$) of the carbonaceous materials.

| Material | $S_{\text{BET}}/$ $\text{m}^2 \text{ g}^{-1}$ | $S_{\text{Non-mic}}/$ $\text{m}^2 \text{ g}^{-1}$ | $V_{\text{Total}}/$ $\text{cm}^3 \text{ g}^{-1}$ | $V_{\text{Mic}}/$ $\text{cm}^3 \text{ g}^{-1}$ | $V_{\text{Mic}}/V_{\text{Total}}$ |
|----------|--|--|---|---|-----------------------------------|
| AC | 850 | 190 | 0.61 | 0.33 | 0.54 |
| CX | 650 | 240 | 1.09 | 0.19 | 0.17 |
| CNT | 248 | 279 | 1.01 | 0.00 | 0.00 |
| GO | 22 | 20 | 0.04 | 0.00 | 0.00 |
| Graphite | 12 | 18 | 0.04 | 0.00 | 0.00 |
| GBCM | 10 | 10 | 0.02 | 0.00 | 0.00 |
| ACS | 850 | 190 | 0.60 | 0.33 | 0.55 |
| ACN | 873 | 196 | 0.61 | 0.31 | 0.52 |
| ACNU | 902 | 218 | 0.61 | 0.31 | 0.52 |
| ACNUT | 1055 | 239 | 0.63 | 0.34 | 0.55 |

The surface acid-base chemical properties of the carbon materials were also determined, the corresponding values being gathered in Table 2. It can be seen that AC and CX possess an evident basic character, with a concentration of basic functionalities higher than the concentration of acidic functionalities and a *PZC* above 7. CNT also have a basic character, with a *PZC* of 8.1, but in this case possessing a concentration of acidic functionalities larger than the concentration of basic functionalities, suggesting the presence of strong basic functional groups and weak acidic functional groups. In contrast, GBCM, due to the presence of high amounts of sulphonic acid groups, is characterized as a strong solid acid carbon material [19], as revealed by its low *PZC* value of 1.3. GO, although possessing an undefined concentration of acidic functionalities due to its partial decomposition occurring in the basic conditions used for the determination of this parameter [32], also shows a pronounced acidic nature, as revealed by a low *PZC* value of 2.8. Graphite presents a slightly acidic character,

with a concentration of acidic functionalities higher than the concentration of basic functionalities and a *PZC* value of 5.5.

Table 2. Acid-base properties ($\pm 10 \mu\text{mol g}^{-1}$) and point of zero charge (*PZC*, ± 0.1) of the carbonaceous materials.

| Material | <i>PZC</i> | Acidity/ $\mu\text{mol g}^{-1}$ | Basicity/ $\mu\text{mol g}^{-1}$ |
|----------|------------|------------------------------------|-------------------------------------|
| AC | 7.6 | 360 | 530 |
| CX | 9.2 | 410 | 490 |
| CNT | 8.1 | 400 | 80 |
| GO | 2.8 | (a) | 0.0 |
| Graphite | 5.5 | 190 | 140 |
| GBCM | 1.3 | (b) | 4.0 |
| ACS | 2.0 | 1000 | 190 |
| ACN | 1.6 | 2300 | 220 |
| ACNU | 6.1 | 1240 | 500 |
| ACNUT | 10.3 | 530 | 890 |

(a) GO partially decomposes under strong alkaline conditions, since the contact with a base promotes decarboxylation of GO sheets [33].

(b) GBCM is an unstable material under basic conditions and partially decomposes.

As expected, the materials resulting from the chemical treatments of AC with concentrated sulphuric acid and with concentrated nitric acid exhibit a pronounced acidic character, with *PZC* values in the range 1.6 to 2.0. The introduction of nitrogen containing functionalities, upon chemical treatment with urea, increases the *PZC* of the resulting material (ACNU) up to values near the neutrality, followed by a substantial decrease of acidic active sites and a large increase of basic active sites; the subsequent thermal treatment promotes the removal of acidic active sites by thermal decomposition and enables the production of a material with a high concentration of basic active sites (ACNUT), which gives it a markedly basic character (*PZC*

value of 10.3). These results are in line with those obtained by TPD (Table 3), where it is possible to confirm that ACNUT is the material with the lowest concentration of oxygen-containing functionalities decomposing as CO and CO₂, while in the opposite, ACN is that with the highest concentration.

Table 3. Concentration of oxygen containing functionalities ($\pm 20 \mu\text{mol g}^{-1}$) released as CO and CO₂ during TPD of the activated carbon materials subjected to different liquid phase treatments.

| Material | CO/ $\mu\text{mol g}^{-1}$ | CO ₂ / $\mu\text{mol g}^{-1}$ | CO/ CO ₂ | % O |
|----------|-------------------------------|---|------------------------|------|
| AC | 1242 | 345 | 3.6 | 3.1 |
| ACS | 2010 | 655 | 3.1 | 5.3 |
| ACN | 4393 | 2369 | 1.9 | 14.6 |
| ACNU | 2870 | 1455 | 2.0 | 9.2 |
| ACNUT | 445 | 119 | 3.7 | 1.1 |

Analysing the values in Table 2 in more detail, it is also clear that all the modified carbon materials present higher values of acidic active sites when compared to the original AC. This suggests that the number of available electrons is lower on the carbon surface of the modified materials, since most of the oxygen-containing functionalities on the surface have an electron withdrawal capacity [9], resulting in the confinement of electron density on the oxygen functionalities and consequent increase of the acidity on the neat graphene basal planes of the activated carbon. Furthermore, it is expected that the number of available electron donating active sites decreases with the increase of acidic functionalities, since these functional groups are generated in the same active sites by capture of the available electrons [34]. The influence of the concentration of oxygen-containing functionalities on the hydrogen peroxide decomposition activity of these materials will be later explored in section 3.2.1.

3.2. Catalytic decomposition of H_2O_2

Screening experiments were carried out to evaluate the ability of the carbon materials (AC, CX, CNT, GO, graphite and GBCM) to act as catalysts in H_2O_2 decomposition. The corresponding results, obtained under the typical conditions referred in Section 2.4, are collected in Figure 1. The best performing material is AC, able to decompose 63% of the initial H_2O_2 content after 150 min of reaction, by far superior to the other materials, which never exceeded 4% H_2O_2 decomposition extent after the same period of time. The results obtained are in line with those recently reported in the literature, concluding about the positive relationship between catalytic activity in H_2O_2 decomposition and the disorder in the structure of the carbon materials, normally associated with less developed graphene layers, higher microporous texture and more available electrons [35], since H_2O_2 decomposition involves the transference of electrons from the carbon surface to the molecule, in order to be reduced [36]. The higher catalytic activity of AC for H_2O_2 decomposition, compared to the catalytic activities of the other tested carbon materials, is thus explained by the microporous nature and the highly disorganized structure of this material, resulting in higher amount of unsaturated carbon atoms, which are usually associated with high concentrations of unpaired electrons [37]. Furthermore, AC has a significantly larger S_{BET} compared to the other tested carbon materials (*cf.* Table 1), also resulting in a larger number of electron donating active sites available for H_2O_2 decomposition.

However, as mentioned in Section 2.2, AC contains Fe in its composition (0.02 wt.%). Bearing this in mind, it would be reasonable to argue that leaching of Fe species into solution may contribute to the observed activity, since it is well known that Fe ions are very active catalysts in CWPO (Fenton process) [34]. In the run performed with AC under typical conditions, the maximum amount of Fe that could be leached into the solution would never exceed 0.02 mg L^{-1} (a hundredfold lower than the allowed limits by European Union

Directives for treated water). Thus, the possible effect of homogeneous catalysis promoted by this amount of Fe was simulated using a Fe^{3+} solution with the same concentration, and maintaining the other parameters with the same values as defined for typical conditions. The decomposition of H_2O_2 obtained under these conditions was negligible, since it is below 3% after 150 min of reaction.

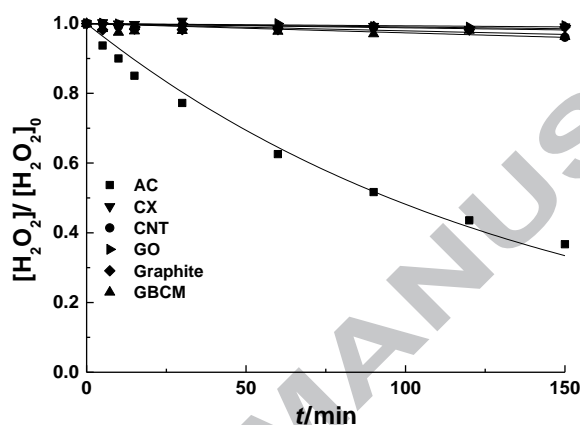


Figure 1. H_2O_2 decomposition obtained in runs performed under typical conditions ($T = 323 \text{ K}$, $\text{pH} = 3$, $[\text{H}_2\text{O}_2]_0 = 34.6 \text{ mmol L}^{-1}$ and catalyst load = 0.1 g L^{-1}) with the six types of carbon materials initially considered (AC, CX, CNT, GO, graphite and GBCM). Points represent experimental data, while lines represent the kinetic model described by Equation 1.

3.2.1. Influence of surface chemistry

As observed, amongst the materials initially tested, AC exhibits inherent properties that are the most relevant for the H_2O_2 catalytic decomposition process. Thus, in order to improve the performance of the activated carbons, it is of interest to study the influence of their surface chemistry on the H_2O_2 catalytic decomposition. For that purpose, two different chemical modification approaches were followed. First, ACS was produced by chemical treatment of AC with concentrated sulphuric acid, since this methodology is able to introduce sulphur containing functional groups onto the carbon surface [6], which are known to increase the

efficiency of CWPO processes [25]. Second, efforts were made to produce a carbon material with a markedly basic character, like ACNUT, since several authors reported carbon materials with basic character as more active for H_2O_2 decomposition in CWPO processes [7-9, 29]. This last methodology is able to introduce nitrogen containing functional groups onto the carbon surface [20], which are also known to increase the extent of H_2O_2 decomposition [39].

The modified activated carbon materials were tested in H_2O_2 decomposition, the corresponding results being given in Figure 2. For comparison purposes, the H_2O_2 decomposition curve obtained in the run performed with the original AC is also given. It is observed that, under the typical conditions, ACS presents practically the same catalytic activity for H_2O_2 decomposition as the original AC, whereas all the other modified carbon materials exhibit lower performances, with catalytic activities following the sequence $\text{ACNUT} > \text{ACNU} > \text{ACN}$. The catalytic activities of AC, ACN, ACNU and ACNUT are in line with the discussion in Section 3.1, since they follow the opposite sequence of their acidic active sites content (*cf.* Table 2), *i.e.*, the catalytic activity is higher for materials with less oxygen-containing functionalities.

In an apparent contradiction to the previous discussion, the ACS material reveals higher catalytic activity than ACNUT, and similar catalytic activity to AC, in spite of its higher concentration of acidic active sites. This fact, which becomes quite evident when the apparent H_2O_2 global decomposition rate constant (k_d) is plotted against the concentration of acidic active sites of the catalysts (*cf.* Figure 3), can be explained by the role of sulphur containing functional groups in the catalytic H_2O_2 decomposition process, as discussed in a previous work [25]. These observations suggest that the acidic functionalities present at carbon surfaces cannot be analysed only in terms of quantity, but also by their quality.

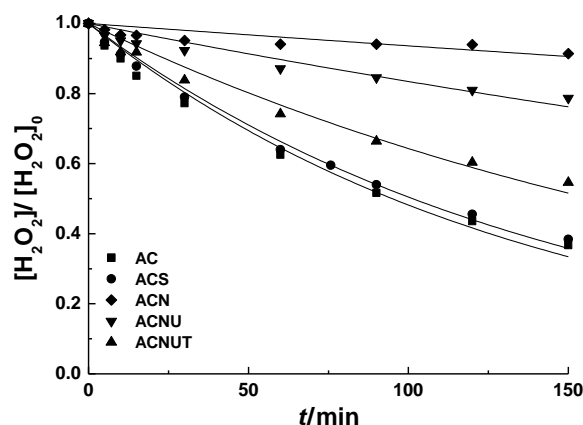


Figure 2. H_2O_2 decomposition obtained in runs performed under typical conditions ($T = 323 \text{ K}$, $\text{pH} = 3$, $[\text{H}_2\text{O}_2]_0 = 34.6 \text{ mmol L}^{-1}$ and catalyst load = 0.1 g L^{-1}) with the original AC and with the modified activated carbons ACS, ACN, ACNU and ACNUT. Points represent experimental data, while lines represent the kinetic model described by Equation 1.

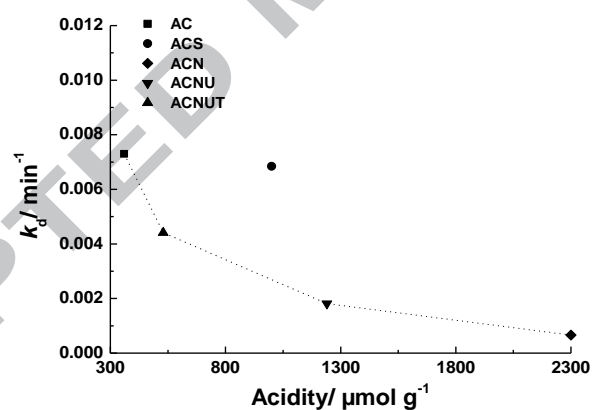


Figure 3. Apparent H_2O_2 global decomposition rate constant (k_d) obtained after 150 min in runs performed under typical conditions ($T = 323 \text{ K}$, $\text{pH} = 3$, $[\text{H}_2\text{O}_2]_0 = 34.6 \text{ mmol L}^{-1}$ and catalyst load = 0.1 g L^{-1}) with the original AC and with the modified activated carbons ACS, ACN, ACNU and ACNUT vs. their concentration of acidic active sites.

3.2.2. Influence of operating conditions

The three catalysts with higher catalytic activity for H_2O_2 decomposition under the typical conditions (*i.e.*, AC, ACS and ACNUT) were selected for further studies, namely to study the influence of the operating conditions on the decomposition of H_2O_2 . For that purpose, the effects of temperature, pH and catalyst load on their performances were considered individually, maintaining the other parameters with the same values as defined for typical conditions.

The effect of reaction temperature was studied in the range 303 K to 343 K and the corresponding apparent H_2O_2 global decomposition rate constants (k_d) are given in Figure 4a. With all catalysts, it is observed that the reaction rate increases as a consequence of increasing the temperature and, whatever the temperature considered, the relative activity sequence of the materials remains the same, *i.e.* $\text{AC} > \text{ACS} > \text{ACNUT}$. It is also observed that ACNUT presents the lowest increase in activity with increasing temperature, reflecting the relative lower activity of this material compared to AC and ACS, which is magnified at higher temperatures. Furthermore, the apparent activation energies (E_a) obtained for the catalytic H_2O_2 decomposition with the studied activated carbons range between 16.4 kJ mol^{-1} and 23.6 kJ mol^{-1} , which are in line with the values reported in literature for other catalysts [39-41].

It is well known that a carbon surface may have both negatively and positively charged sites, depending on the solution pH. At some pH – the point of zero charge (*PZC*) – the overall surface charge will be zero, but for pH values below the *PZC*, the surface will be covered by protonated groups [37, 42]. Thus, solution pH strongly affects the nature of the carbon surface, becoming therefore an important variable for further analysis. The effect of solution pH was studied performing H_2O_2 decomposition experiments under the typical conditions, except the pH, which was varied in the range 3 to 9. The apparent H_2O_2 global

decomposition rate constants (k_d) obtained with AC, ACS and ACNUT at different solution pHs are given in Figure 4b. Similarly to the effect of operating temperature, increasing pH in the range studied favours H_2O_2 decomposition, regardless of the activated carbon catalyst considered. Nevertheless, a deeper analysis of Figure 4b reveals that the increase of H_2O_2 decomposition with increase of pH observed with each carbon material is qualitatively different. For example, the H_2O_2 decomposition rate achieved when using AC as catalyst is the highest amongst the three materials at pH = 3; but the same material presents the lowest H_2O_2 decomposition rate when the pH is increased. This observation, together with the behaviours of ACS and ACNUT in this study, contradicts the explanation which considers that H_2O_2 decomposition is mainly due to its dissociation as weak acid, favoured at higher pH, as reported in previous works [43, 44]. In face of this theory, it would be reasonable to expect that the behaviour of the catalysts would be a direct consequence of their *PZC* [29, 35]. However, the differences in the surface chemistry of ACS and ACNUT (*cf.* Table 2), along with the results in Figure 4b, suggest that the acidic or basic nature of the carbon surface is unable, by itself, to determine the extent to which H_2O_2 is decomposed. In fact, the results suggest that both sulphur containing and nitrogen containing functional groups may be the key factor in establishing differences between H_2O_2 decomposition rates observed in the pH range studied. From a global analysis of the results in Figure 4b, it can be concluded that ACS reveals the best performance in the decomposition of H_2O_2 in most of the pH range studied, thus being regarded as the potentially most interesting metal-free carbon catalyst for H_2O_2 removal from wastewaters.

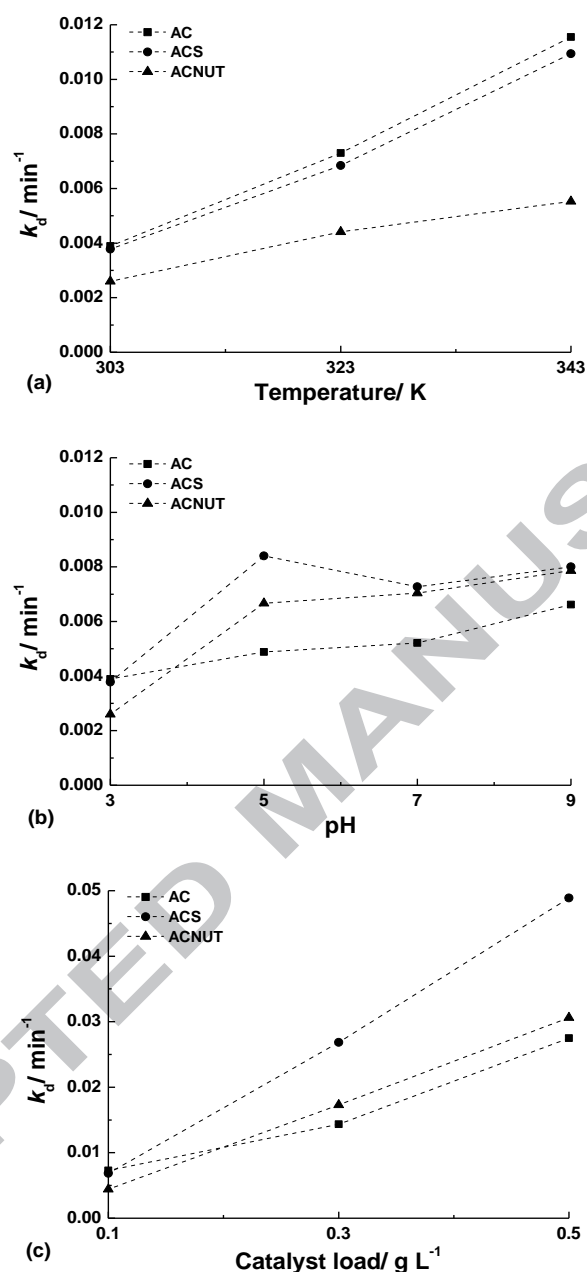


Figure 4. Influence of temperature (a), pH (b) and catalyst load (c) on the apparent H_2O_2 global decomposition rate constant (k_d) obtained in runs performed with AC, ACS and ACNUT.

Finally, to assess the ability of AC, ACS and ACNUT to promote the complete H_2O_2 decomposition, some experiments with increased catalyst load were also performed under the typical conditions, except the catalyst load, which was varied in the range 0.1 g L^{-1} to

0.5 g L⁻¹. The apparent H₂O₂ global decomposition rate constants (k_d) obtained with different catalyst loads are given in Figure 4c, putting in evidence the superior performance of ACS. As expected, increasing catalyst load increases H₂O₂ decomposition, with almost complete H₂O₂ decomposition being achieved with all tested catalysts after 150 min of reaction when using a catalyst load of 0.5 g L⁻¹, as observed in Table 4, which gathers the results obtained in all H₂O₂ decomposition experiments performed under the different operating conditions reported in this section, in terms of H₂O₂ decomposition extent after 150 min ($X_{H_2O_2}$).

Table 4. H₂O₂ decomposition ($X_{H_2O_2}$) obtained after 150 min in runs performed with AC, ACS and ACNUT under different operating conditions.

| Catalyst load/ g L ⁻¹ | pH | Temperature/ K | $X_{H_2O_2}/ \%$ | | |
|----------------------------------|----|----------------|------------------|-----|-------|
| | | | AC | ACS | ACNUT |
| 0.1 | 3 | 303 | 43 | 42 | 30 |
| 0.1 | 3 | 323 | 63 | 62 | 45 |
| 0.1 | 3 | 343 | 78 | 75 | 53 |
| 0.1 | 5 | 323 | 50 | 69 | 60 |
| 0.1 | 7 | 323 | 55 | 65 | 64 |
| 0.1 | 9 | 323 | 62 | 68 | 68 |
| 0.3 | 3 | 323 | 88 | 98 | 93 |
| 0.5 | 3 | 323 | 99 | 100 | 99 |

3.2.3. Reutilization studies

In the previous section, ACS was found to perform better than AC and ACNUT in the majority of the conditions studied. Accordingly, it was selected for reutilization studies performing a series of three consecutive H₂O₂ decomposition runs, considering $T = 323$ K, $pH = 3$, $[H_2O_2]_0 = 34.6$ mmol L⁻¹ and catalyst load = 0.5 g L⁻¹. After each run, the catalyst was filtered, washed and dried overnight at 333 K, and then reused with a fresh H₂O₂ solution. The aim of this study was to assess the catalyst stability for the H₂O₂ decomposition process, a basic requirement for its application at the industrial scale.

The results obtained in this series of experiments, in terms of H_2O_2 decomposition curves, are given in Figure 5. As expected, it can be observed that H_2O_2 decomposition is faster in the first run when compared to the second run, due to the possible oxidation of some active sites at the carbon surface. Nevertheless, the differences between the second and third run are less significant, suggesting that ACS may be an active and stable catalyst for the removal of H_2O_2 in aqueous solutions at the industrial scale.

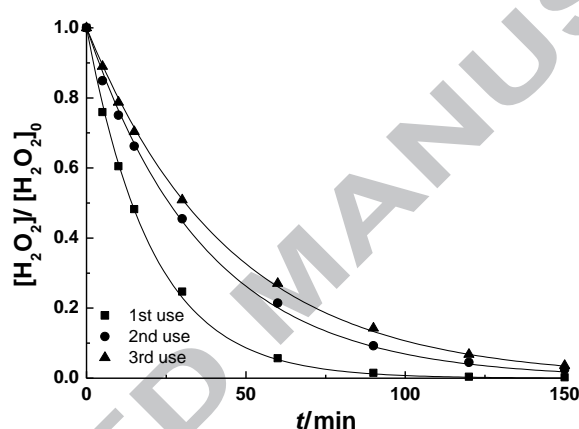


Figure 5. H_2O_2 decomposition obtained in a series of three consecutive runs, considering the reuse of ACS at $T = 323$ K, $\text{pH} = 3$, $[\text{H}_2\text{O}_2]_0 = 34.6$ mmol L^{-1} and catalyst load = 0.5 g L^{-1} . Points represent experimental data, while lines represent the kinetic model described by Equation 1.

3.3. Mechanistic interpretation of H_2O_2 decomposition

So far in this work, the reported H_2O_2 decomposition experiments using carbon materials as catalysts have only been performed by monitoring the decrease of H_2O_2 concentration. However, the mechanism associated to the decomposition of H_2O_2 is quite complex, involving the generation of various intermediate species, including the generation of highly reactive HO^\bullet [26, 45], which justifies the importance and the efforts on research and

development of carbon materials as catalysts for CWPO of organic pollutants [2, 9, 31]. Thus, it is of utmost importance to quantify the ability of the catalysts to promote the decomposition of H_2O_2 via formation of HO^\bullet . For that purpose, the yield of HO^\bullet formed during the H_2O_2 decomposition process was obtained considering the following mechanism for H_2O_2 decomposition (Table 5), which is based on a literature survey [26, 29, 30, 35, 38, 46-53]:

- $[\text{H}_2\text{O}_2]$ can be decomposed via HO^\bullet formation, with the participation of reducing active sites $[\text{S}]$ existing at the carbon surface (Equation 2);
- Hydrogen peroxide $[\text{H}_2\text{O}_2]$ adsorbed over the oxidized active sites $[\text{S}^+]$ can be decomposed to hydroperoxyl radicals (HOO^\bullet) and a proton (H^+) regenerating $[\text{S}]$ (Equation 3);
- Adsorbed hydroperoxyl radicals (HOO^\bullet) and a proton (H^+) can produce atomic oxygen (which may remain trapped in the surface and account for the formation of carbon surface oxides) and water when in contact with reducing active sites $[\text{S}]$ existing at the carbon surface (Equation 4);
- Due to self-annihilation, H_2O_2 in the bulk can be decomposed to HOO^\bullet , HO^\bullet , O_2 and water, by reacting with formed HOO^\bullet , HO^\bullet and $\text{O}_2^{\bullet-}$ (Equations 6-8). Because of the low bimolecular rate, equations 7 and 8 will have a negligible contribution to this self-annihilation process. H_2O_2 in the bulk may also be decomposed through its dissociation as a weak acid (Equation 5).
- Finally, the radicals HO^\bullet , HOO^\bullet and $\text{O}_2^{\bullet-}$ can react with themselves resulting mainly in O_2 , water and some minor amounts of regenerated H_2O_2 (Equations 10-16), or in the case of HOO^\bullet , decomposing by a first order process (Equation 9).

Most of the reactions included in Table 5 (Equations 6-16) are extensively accepted in AOPs [54, 55], in addition to the catalytic surface reactions (Equations 2-4).

Table 5. Reaction mechanisms for H₂O₂ decomposition.

| Reaction | Comment / Rate |
|---|--|
| $[\text{H}_2\text{O}_2 + \text{S}] \rightarrow \text{HO}^\bullet + \text{OH}^- + [\text{S}^+]$ | This study (2) |
| $[\text{H}_2\text{O}_2 + \text{S}^+] \rightarrow \text{HOO}^\bullet + \text{H}^+ + [\text{S}]$ | This study (3) |
| $[\text{HOO}^\bullet + \text{H}^+ + \text{S}] \rightarrow \text{H}_2\text{O} + [\text{O}^\bullet + \text{S}^+]$ | This study (4) |
| $\text{H}_2\text{O}_2 \rightleftharpoons \text{H}^+ + \text{HO}_2^-$ | pKa = 11.75 [50] (5) |
| $\text{H}_2\text{O}_2 + \text{HO}^\bullet \rightarrow \text{H}_2\text{O} + \text{HOO}^\bullet$ | $2.7 \times 10^7 \text{ M}^{-1} \text{ s}^{-1}$ [47] (6) |
| $\text{H}_2\text{O}_2 + \text{HOO}^\bullet \rightarrow \text{HO}^\bullet + \text{H}_2\text{O} + \text{O}_2$ | $3 \text{ M}^{-1} \text{ s}^{-1}$ [51] (7) |
| $\text{H}_2\text{O}_2 + \text{O}_2^{\bullet -} \rightarrow \text{HO}^\bullet + \text{OH}^- + \text{O}_2$ | $0.13 \text{ M}^{-1} \text{ s}^{-1}$ [53] (8) |
| $\text{HOO}^\bullet \rightarrow \text{O}_2^{\bullet -} + \text{H}^+$ | $1.58 \times 10^5 \text{ s}^{-1}$ [46] (9) |
| $\text{O}_2^{\bullet -} + \text{H}^+ \rightarrow \text{HOO}^\bullet$ | $1 \times 10^{10} \text{ M}^{-1} \text{ s}^{-1}$ [46] (10) |
| $\text{HO}_2^- + \text{HO}^\bullet \rightarrow \text{HOO}^\bullet + \text{OH}^-$ | $7.5 \times 10^9 \text{ M}^{-1} \text{ s}^{-1}$ [48] (11) |
| $\text{HO}^\bullet + \text{HOO}^\bullet \rightarrow \text{H}_2\text{O} + \text{O}_2$ | $6.6 \times 10^9 \text{ M}^{-1} \text{ s}^{-1}$ [49] (12) |
| $\text{HO}^\bullet + \text{HO}^\bullet \rightarrow \text{H}_2\text{O}_2$ | $5.5 \times 10^9 \text{ M}^{-1} \text{ s}^{-1}$ [47] (13) |
| $\text{HOO}^\bullet + \text{HOO}^\bullet \rightarrow \text{H}_2\text{O}_2 + \text{O}_2$ | $8.3 \times 10^5 \text{ M}^{-1} \text{ s}^{-1}$ [46] (14) |
| $\text{HO}^\bullet + \text{O}_2^{\bullet -} \rightarrow \text{OH}^- + \text{O}_2$ | $8 \times 10^9 \text{ M}^{-1} \text{ s}^{-1}$ [52] (15) |
| $\text{HOO}^\bullet + \text{O}_2^{\bullet -} \rightarrow \text{HO}_2^- + \text{O}_2$ | $9.7 \times 10^7 \text{ M}^{-1} \text{ s}^{-1}$ [46] (16) |

It is clear from the proposed mechanism that the experiments that monitor only the concentration of H₂O₂, such as those reported so far, are not enough to determine the amount of HO[•] formed, since H₂O₂ decomposition may proceed either via HO[•] formation on the surface (as described by Equation 2) and in the bulk (Equations 7 and 8), or via other species (as described by Equations 3, 5 and 6); thus, further studies were planned in order to achieve the desired objective, namely to obtain the yield of HO[•] formed during the H₂O₂ decomposition process using the three catalysts with higher activity for H₂O₂ decomposition

under the typical conditions (AC, ACS and ACNUT, *cf.* Section 3.2.1). Bearing this in mind, a new set of H₂O₂ decomposition experiments was performed, in which the amount of oxygen formed was monitored. In addition, two other separate sets of experiments were performed, namely the decomposition of H₂O₂ in which the concentration of H₂O₂ was monitored, and the decomposition of H₂O₂ in which the amount of oxygen formed was monitored, using methanol (MeOH) as HO[•] scavenger, a fast reaction that proceeds as schematically indicated in Equation 17 [26, 56].



Accordingly, when MeOH is used, the H₂O₂ decomposition mechanism proceeds mainly by Equations 2-4 and 17. Since the reaction of MeOH with HOO[•] or O₂^{•-} is known to occur very slowly and these radicals are in very minute concentrations according to the kinetics indicated in Table 5, no significant interference occurs in the amount of oxygen formed through the reactions described by Equations 3 and 4 [38, 57] and, as the reaction given by Equations 12-16 will not be important in the presence of MeOH, it can be assumed that the difference between the oxygen formed in the H₂O₂ decomposition experiments performed with and without MeOH is equivalent to the amount of HO[•] formed along the process. Likewise, the difference between the H₂O₂ consumption in the H₂O₂ decomposition experiments performed with and without MeOH can be attributed to the H₂O₂ self-annihilation reaction described by Equation 6.

Taking into consideration the previous observations, the yield of HO[•] formed during the H₂O₂ decomposition process ($Y_{\text{HO}^{\bullet}}$) can be evaluated using Equation 18, where $n_{\text{HO}^{\bullet}}$ represents the moles of HO[•] formed during the H₂O₂ decomposition process, obtained by the difference between the oxygen formed in the H₂O₂ decomposition experiments performed

with and without MeOH, and $n_{\text{H}_2\text{O}_2, \text{MeOH}}$ represents the moles of H_2O_2 consumed during the H_2O_2 decomposition experiment performed with MeOH, which is equivalent to the maximum amount of HO^\bullet that could be formed, by Equations 2, 7 and 8, from the effectively decomposed H_2O_2 .

$$Y_{\text{HO}^\bullet}/\% = \frac{n_{\text{HO}^\bullet}}{n_{\text{H}_2\text{O}_2, \text{MeOH}}} \times 100 \quad (18)$$

The results obtained in all H_2O_2 decomposition experiments performed with AC, ACS and ACNUT (either monitoring the concentration of H_2O_2 or the amount of oxygen formed, with and without MeOH) are shown in Figure 6a, b and c, respectively. From a first analysis of the results, it is concluded that the proposed mechanism is supported by the experimental data. For instance, the H_2O_2 self-annihilation promoted by formed HO^\bullet , as described by Equation 6, is quite significant when AC is used as catalyst, being negligible when ACNUT is considered; *i.e.* the differences in H_2O_2 decay between the experiments performed with and without MeOH are relevant for AC (Figure 6a), indicating that the reaction described by Equation 6 prevails, while they are negligible for ACNUT (Figure 6c), suggesting that the reactions described by Equations 3, 4 and 9-16 prevail in opposition to the self-annihilation of H_2O_2 shown in Equation 6. On the contrary, the largest difference between the oxygen formed in the H_2O_2 decomposition experiments performed with and without MeOH is observed when ACNUT is used as catalyst, suggesting that ACNUT, although not showing the highest catalytic activity for the global decomposition of H_2O_2 , is the catalyst with the highest selectivity for the decomposition of H_2O_2 via formation of HO^\bullet , as described by Equation 2. In order to confirm these observations, the yield of HO^\bullet formed during the H_2O_2

decomposition process ($Y_{HO\cdot}$) was evaluated using Equation 18, as previously described. The corresponding results are gathered in Table 6.

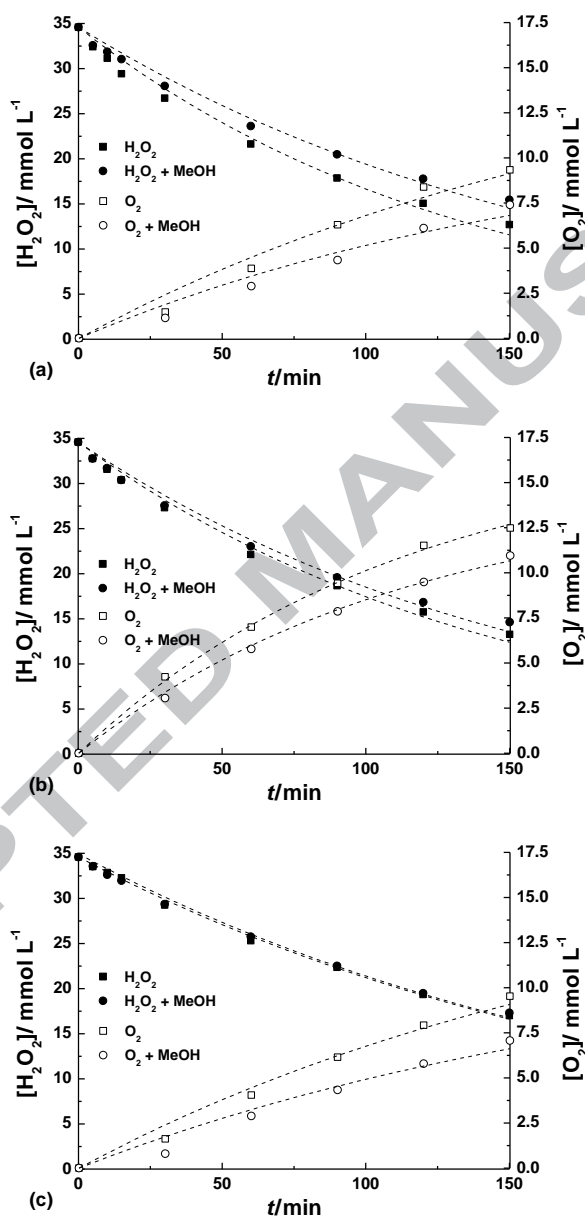


Figure 6. H_2O_2 decomposition (filled symbols) and oxygen formation (open symbols) during H_2O_2 decomposition experiments performed under typical conditions ($T = 323$ K, $pH = 3$, $[H_2O_2]_0 = 34.6$ $mmol L^{-1}$ and catalyst load = 0.1 $g L^{-1}$) with AC (a), ACS (b) and ACNUT (c). Experiments performed with (circles) and without (squares) MeOH (20 $g L^{-1}$). Points represent experimental data, while lines represent the kinetic model described by Equation 1.

From the results in Table 6, it is clear that all the tested materials are able to act as catalysts in the H_2O_2 decomposition via HO^\bullet formation. The highest Y_{HO^\bullet} amongst the tested materials is obtained when using ACNUT as catalyst and the Y_{HO^\bullet} values follow the order $\text{ACNUT} > \text{AC} > \text{ACS}$. This order is in accordance with the concentration of basic active sites at the surface of the materials (*cf.* Table 2), suggesting that the basicity of carbon materials increases the yield of HO^\bullet formation, which may be explained by the reducing character of basic groups, necessary condition for the promotion of the reaction described by Equation 2, which is in line with other results published in literature [35, 44, 58]. This relationship is clearly visible when Y_{HO^\bullet} is plotted against the concentration of basic active sites at the surface of the carbon materials (*cf.* Figure 7), where the existence of a linear correlation becomes evident.

Table 6. Yield of HO^\bullet formed during the H_2O_2 decomposition process (Y_{HO^\bullet}) and related parameters, obtained after 150 min in H_2O_2 decomposition experiments performed under typical conditions ($T = 323$ K, $\text{pH} = 3$, $[\text{H}_2\text{O}_2]_0 = 34.6$ mmol L^{-1} and catalyst load = 0.1 g L^{-1}) with AC, ACS and ACNUT. Experiments performed with and without MeOH (20 g L^{-1}).

| Material | Parameter | | |
|----------|---|---------------------------------------|------------------------------|
| | $n_{\text{H}_2\text{O}_2, \text{MeOH}} / \text{mmol}$ | $n_{\text{HO}^\bullet} / \text{mmol}$ | $Y_{\text{HO}^\bullet} / \%$ |
| AC | 4.9 | 0.50 | 10 |
| ACS | 5.1 | 0.39 | 7.7 |
| ACNUT | 4.4 | 0.63 | 14 |

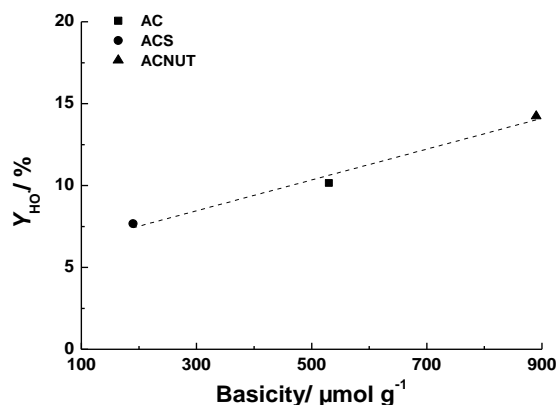


Figure 7. Yield of $\text{HO}\cdot$ formed during the H_2O_2 decomposition process ($Y_{\text{HO}\cdot}$) obtained after 150 min in runs performed under typical conditions ($T = 323 \text{ K}$, $\text{pH} = 3$, $[\text{H}_2\text{O}_2]_0 = 34.6 \text{ mmol L}^{-1}$ and catalyst load = 0.1 g L^{-1}) with the original AC and with the modified activated carbons ACS and ACNUT vs. their concentration of basic active sites. Points represent experimental data, while line represents the linear fitting ($r^2 = 0.97$).

4. Conclusions

Amongst the tested carbon materials, characterized by different structural and chemical properties, the classical activated carbons are found to be the best solution for the non-selective decomposition of H_2O_2 in aqueous solutions.

In particular, the material resulting from the treatment of the original activated carbon with concentrated sulphuric acid (ACS) presents the highest catalytic activity in the majority of the reaction conditions studied, with the observed activity being attributed to the presence of sulphur containing functional groups at the materials surface.

By proper selection of the reaction conditions, ACS was found as a very effective material for the decomposition of H_2O_2 , since the complete removal of H_2O_2 could be achieved.

Further reutilization studies suggest that ACS may also be a stable catalyst for the removal of H_2O_2 in aqueous solutions at the industrial scale.

In order to quantify the ability of the catalysts to promote the decomposition of H_2O_2 via formation of HO^\bullet , a reaction mechanism was proposed, considering this pathway in parallel with the decomposition of H_2O_2 via other species, allowing the interpretation of the experimental data.

Accordingly, ACNUT – an activated carbon material with a markedly basic character – led to the highest yield of HO^\bullet formed during the H_2O_2 decomposition process (14% at the typical reaction conditions). Furthermore, the results obtained suggest that the basicity of carbon materials enhances the yield of HO^\bullet formation.

In summary, it is concluded that sulphur containing functional groups at the surface of activated carbons promote the non-selective decomposition of H_2O_2 in aqueous solutions, while the selective decomposition of H_2O_2 via HO^\bullet formation is favoured by basic active sites on the surface of activated carbons.

Acknowledgments

Work supported by project PTDC/AAC-AMB/110088/2009 and partially by project PEst-C/EQB/LA0020/2011, financed by FEDER through COMPETE - Programa Operacional Factores de Competitividade and by FCT - Fundação para a Ciência e a Tecnologia.

References

- [1] USATSDR. Medical management guidelines for hydrogen peroxide. Atlanta, US; 2011.
- [2] Gogate PR, Pandit AB. A review of imperative technologies for wastewater treatment I: oxidation technologies at ambient conditions. *Adv Environ Res* 2004; 8(3-4):501-51.
- [3] Hage R, Lienke A. Applications of transition-metal catalysts to textile and wood-pulp bleaching. *Angew Chem Int Ed* 2006; 45(2):206-22.

- [4] Raffellini S, Schenk M, Guerrero S, Alzamora SM. Kinetics of *Escherichia coli* inactivation employing hydrogen peroxide at varying temperatures, pH and concentrations. *Food Contr* 2011; 22(6):920-32.
- [5] Jones CW. Applications of hydrogen peroxide and derivatives. Cambridge, UK: The Royal Society of Chemistry; 1999.
- [6] Gomes HT, Miranda SM, Sampaio MJ, Silva AMT, Faria JL. Activated carbons treated with sulphuric acid: catalysts for catalytic wet peroxide oxidation. *Catal Today* 2010; 151(1-2):153-8.
- [7] Lücking F, Köser H, Jank M, Ritter A. Iron powder, graphite and activated carbon as catalysts for the oxidation of 4-chlorophenol with hydrogen peroxide in aqueous solution. *Water Res* 1998; 32(9):2607-14.
- [8] Ribeiro RS, Fathy NA, Attia AA, Silva AMT, Faria JL, Gomes HT. Activated carbon xerogels for the removal of the anionic azo dyes Orange II and Chromotrope 2R by adsorption and catalytic wet peroxide oxidation. *Chem Eng J* 2012; 195-196:112-21.
- [9] Santos VP, Pereira MFR, Faria PCC, Órfão JJM. Decolourisation of dye solutions by oxidation with H_2O_2 in the presence of modified activated carbons. *J Hazard Mat* 2009; 162(2-3):736-42.
- [10] Navalon S, Dhakshinamoorthy A, Alvaro M, Garcia H. Heterogeneous Fenton catalysts based on activated carbon and related materials. *ChemSusChem* 2011; 4(12):1712-30.
- [11] Zazo JA, Casas JA, Mohedano AF, Rodríguez JJ. Catalytic wet peroxide oxidation of phenol with a Fe/active carbon catalyst. *Appl Catal B Environ* 2006; 65(3-4):261-8.
- [12] Gomes HT, Machado BF, Ribeiro A, Moreira I, Rosário M, Silva AMT, et al. Catalytic properties of carbon materials for wet oxidation of aniline. *J Hazard Mat* 2008; 159(2-3):420-6.
- [13] Arkema. Graphistrength[®] C100 data sheet for product development. France; 2006.

- [14] Huang LW, Elkedim O, Nowak M, Jurczyk M, Chassagnon R, Meng DW. Synergistic effects of multiwalled carbon nanotubes and Al on the electrochemical hydrogen storage properties of Mg₂Ni type alloy prepared by mechanical alloying. *Int J Hydrogen Energy* 2012; 37(2):1538-45.
- [15] Sigma-Aldrich. Multi-walled carbon nanotubes (ref. 677248) material safety data sheet, Version 5.0. St. Louis MO, US; 2013.
- [16] Hummers WS, Offeman RE. Preparation of Graphitic Oxide. *J Am Chem Soc* 1958; 80(6):1339-39.
- [17] Stankovich S, Dikin DA, Piner RD, Kohlhaas KA, Kleinhammes A, Jia Y, *et al.* Synthesis of graphene-based nanosheets via chemical reduction of exfoliated graphite oxide. *Carbon* 2007; 45(7):1558-65.
- [18] Pastrana-Martínez LM, Morales-Torres S, Likodimos V, Figueiredo JL, Faria JL, Falaras P, *et al.* Advanced nanostructured photocatalysts based on reduced graphene oxide-TiO₂ composites for degradation of diphenhydramine pharmaceutical and methyl orange dye. *Appl Catal B Environ* 2012; 123-124:241-56.
- [19] Prabhavathi Devi BLA, Gangadhar KN, Sai Prasad PS, Jagannadh B, Prasad RBN. A Glycerol-based carbon catalyst for the preparation of biodiesel. *ChemSusChem* 2009; 2(7):617-20.
- [20] Rocha RP, Sousa JPS, Silva AMT, Pereira MFR, Figueiredo JL. Catalytic activity and stability of multiwalled carbon nanotubes in catalytic wet air oxidation of oxalic acid: The role of the basic nature induced by the surface chemistry. *Appl Catal B Environ* 2011; 104(3-4):330-6.
- [21] Figueiredo JL, Pereira MFR, Freitas MMA, Órfão JJM. Modification of the surface chemistry of activated carbons. *Carbon* 1999; 37(9):1379-89.

- [22] Newcombe G, Hayes R, Drikas M. Granular activated carbon: Importance of surface properties in the adsorption of naturally occurring organics. *Colloids Surf A* 1993; 78: 65-71.
- [23] Ferro-García MA, Rivera-Utrilla J, Bautista-Toledo I, Moreno-Castilla C. Adsorption of humic substances on activated carbon from aqueous solutions and their effect on the removal of Cr(III) Ions. *Langmuir* 1998; 14:1880-6.
- [24] Rivera-Utrilla J, Bautista-Toledo I, Ferro-García MA, Moreno-Castilla C. Activated carbon surface modifications by adsorption of bacteria and their effect on aqueous lead adsorption. *J Chem Technol Biotechnol* 2001; 76(12):1209-15.
- [25] Gomes HT, Miranda SM, Sampaio MJ, Figueiredo JL, Silva AMT, Faria JL. The role of activated carbons functionalized with thiol and sulfonic acid groups in catalytic wet peroxide oxidation. *Appl Catal B Environ* 2011; 106(3-4):390-7.
- [26] Rey A, Bahamonde A, Casas JA, Rodríguez JJ. Selectivity of hydrogen peroxide decomposition towards hydroxyl radicals in catalytic wet peroxide oxidation (CWPO) over Fe/AC catalysts. *Water Sci Tech* 2010; 61(11):2769-78.
- [27] Ketchie WC, Fang Y-L, Wong MS, Murayama M, Davis RJ. Influence of gold particle size on the aqueous-phase oxidation of carbon monoxide and glycerol. *J Catal* 2007; 250(1):94-101.
- [28] Satterfield CN, Bonnell AH. Interferences in titanium sulfate method for hydrogen peroxide. *Anal Chem* 1955; 27(7):1174-5.
- [29] Khalil LB, Girgis BS, Tawfik TAM. Decomposition of H₂O₂ on activated carbon obtained from olive stones. *J Chem Tech Biotechnol* 2001; 76(11):1132-40.
- [30] Lin S-S, Gurol MD. Catalytic decomposition of hydrogen peroxide on iron oxide: kinetics, mechanism, and implications. *Environ Sci Tech* 1998; 32(10):1417-23.
- [31] Navalon S, Alvaro M, Garcia H. Heterogeneous Fenton catalysts based on clays, silicas and zeolites. *Appl Catal B Environ* 2010; 99(1-2):1-26.

- [32] Rourke JP, Pandey PA, Moore JJ, Bates M, Kinloch IA, Young RJ, *et al.* The real graphene oxide revealed: stripping the oxidative debris from the graphene-like sheets. *Angew Chem Int Ed* 2011; 50(14):3173-7.
- [33] Dimiev AM, Alemany LB, Tour JM. Graphene oxide. Origin of acidity, its instability in water, and a new dynamic structural model. *ACS Nano* 2012; 7(1):576-88.
- [34] Serp P, Figueiredo JL. Carbon materials for catalysis. Hoboken, NJ: John Wiley & Sons, Inc; 2009.
- [35] Rey A, Zazo JA, Casas JA, Bahamonde A, Rodríguez JJ. Influence of the structural and surface characteristics of activated carbon on the catalytic decomposition of hydrogen peroxide. *Appl Catal Gen* 2011; 402(1-2):146-55.
- [36] Kimura M, Miyamoto I. Discovery of the activated-carbon radical AC^+ and the novel oxidation-reactions comprising the AC/AC^+ cycle as a catalyst in an aqueous-solution. *Bull Chem Soc Jpn* 1994; 67(9):2357-60.
- [37] Rodríguez-Reinoso F. The role of carbon materials in heterogeneous catalysis. *Carbon* 1998; 36(3):159-75.
- [38] Pignatello JJ, Oliveros E, MacKay A. Advanced oxidation processes for organic contaminant destruction based on the Fenton reaction and related chemistry. *Crit Rev Environ Sci Technol* 2006; 36(1):1-84.
- [39] Voitko KV, Whitby RLD, Gun'ko VM, Bakalinska OM, Kartel MT, Laszlo K, *et al.* Morphological and chemical features of nano and macroscale carbons affecting hydrogen peroxide decomposition in aqueous media. *J Colloid Interface Sci* 2011; 361(1):129-36.
- [40] Hasan MA, Zaki MI, Pasupulety L, Kumari K. Promotion of the hydrogen peroxide decomposition activity of manganese oxide catalysts. *Appl Catal Gen* 1999; 181(1):171-9.
- [41] Paternina E, M. Arias J, Barragán D. Kinetic study of the catalyzed decomposition of hydrogen peroxide on activated carbon. *Quím Nova* 2009; 32:934-8.

- [42] Al-Degs YS, El-Barghouthi MI, El-Sheikh AH, Walker GA. Effect of solution pH, ionic strength, and temperature on adsorption behavior of reactive dyes on activated carbon. *Dyes Pigm* 2008; 77(1):16-23.
- [43] Puri BR, Kalra KC. The decomposition of hydrogen peroxide in the presence of carbon blacks. *Carbon* 1971; 9(3):313-20.
- [44] Strelko V, Stavitskaya S, Tsyba N, Lysenko A, Zhuravskii S, Goba V. Directed modification of carbons of varied origin and chemical nature of the surface in order to control their catalytic activity. *Russ J Appl Chem* 2007; 80(3):389-96.
- [45] Aguinaco A, Pocostales JP, García-Araya JF, Beltrán FJ. Decomposition of hydrogen peroxide in the presence of activated carbons with different characteristics. *J Chem Technol Biotechnol* 2011; 86(4):595-600.
- [46] Bielski BHJ, Cabelli DE, Arudi RL, Ross AB. Reactivity of HO_2/O_2^- radicals in aqueous solution. *J Phys Chem Ref Data* 1985; 14(4):1041-100.
- [47] Buxton GV, Greenstock CL, Helman WP, Ross AB. Critical Review of rate constants for reactions of hydrated electrons, hydrogen atoms and hydroxyl radicals ($\text{HO}^\bullet/\text{O}^\bullet$) in Aqueous Solution. *J Phys Chem Ref Data* 1988; 17(2):513-886.
- [48] Christensen H, Sehested K, Corfitzen H. Reactions of hydroxyl radicals with hydrogen peroxide at ambient and elevated temperatures. *J Phys Chem* 1982; 86(9):1588-90.
- [49] Elliot AJ, Buxton GV. Temperature dependence of the reactions $\text{OH} + \text{O}_2^-$ and $\text{OH} + \text{HO}_2$ in water up to 200 °C. *J Chem Soc Faraday Trans* 1992; 88(17):2465-70.
- [50] Evans MG, Uri N. The dissociation constant of hydrogen peroxide and the electron affinity of the HO_2 radical. *Trans Faraday Soc* 1949; 45:224-30.
- [51] Koppenol WH, Butler J, Van Leeuwen JW. The Haber-Weiss cycle. *Photochem Photobiol* 1978; 28(4-5):655-8.

- [52] Linden KG, Sharpless CM, Andrews SA, Atasi KZ, Korategere V, Stefan M, *et al.* Innovative UV technologies to oxidize organic and organoleptic chemicals. London UK, IWA Publishing; 2005.
- [53] Weinstein J, Bielski BHJ. Kinetics of the interaction of perhydroxyl and superoxide radicals with hydrogen peroxide. The Haber-Weiss reaction. *J Am Chem Soc* 1979; 101(1):58-62.
- [54] Ghafoori S, Mehrvar M, Chan PK. Free-radical-induced degradation of aqueous polyethylene oxide by UV/H₂O₂: experimental design, reaction mechanisms, and kinetic modeling. *Ind Eng Chem Res* 2012; 51(46):14980-93.
- [55] Schaefer T, Schindelka J, Hoffmann D, Herrmann H. Laboratory kinetic and mechanistic studies on the OH-initiated oxidation of acetone in aqueous solution. *J Phys Chem* 2012; 116(24):6317-26.
- [56] Jiménez E, Gilles MK, Ravishankara AR. Kinetics of the reactions of the hydroxyl radical with CH₃OH and C₂H₅OH between 235 and 360 K. *J Photochem Photobiol Chem* 2003; 157(2-3):237-45.
- [57] Miller CM, Valentine RL. Mechanistic studies of surface catalyzed H₂O₂ decomposition and contaminant degradation in the presence of sand. *Water Res* 1999; 33(12):2805-16.
- [58] Castro C, Oliveira L, Guerreiro M. Effect of hydrogen treatment on the catalytic activity of iron oxide based materials dispersed over activated carbon: investigations toward hydrogen peroxide decomposition. *Catal Lett* 2009; 133(1):41-8.